Optimized Line-of-Sight Assessment Algorithm for 5G mmW Network Design using LiDAR Information

Reza Soosahabi and Magdy Bayoumi
Department of Electrical & Computer Engineering, University of Louisiana at Lafayette, Lafayette, LA 70504, U.S.A.

Keywords: 5G-NR, mmW Network Design, Fixed-Wireless Access, Line-of-Sight Assessment, LiDAR Application, Visibility Algorithm.

Abstract: Utilizing mmW carrier frequency bands (aka above-6 GHz) at the network edge, is a key enabling factor to achieve near Gbps throughput in 5G-NR technology. The propagation characteristics of mmW signals in outdoor environment complicates 5G mmW network design. Previously used in backhaul networks, the service availability of mmW radio technologies significantly relies on the Line-of-Sight (LoS) signal path between the communicating radios. LiDAR is considered a popular source of high-resolution aerial survey data suitable for accurate LoS assessment. Maintaining low radio mounting height is another cost-related factor in practical 5G mmW network design. In this work we present a comprehensive LoS assessment problem incorporating radio mounting height. Then we propose a new LoS assessment algorithm using LiDAR data that is computationally optimized for the practical aspects of 5G mmW network design. Empowered by a novel method to topologically sort terrain data, it achieves constant-time, $O(1)$, complexity to execute LoS assessment per user location, whereas the complexity of retrofitted LoS algorithms for the same task grows linearly with respect to the data dimensions. The improvements in the run-time efficiency are verified in numerical results for a real deployment scenario.

1 INTRODUCTION

Superseding the Long-Term Evolution wireless technology, 5G is envisioned to be the prominent unifying connectivity solution for a wide range of applications in the present decade. In terms of mobile and broadband services, it is designed to offer near Gbps throughput over wireless links at extremely low latency. This is achieved by 5G-NR advanced radios utilizing transmission bandwidths in the scale of hundreds of MHz available in millimeter-wave (mmW) carrier frequency bands (aka above-6 GHz) as well as other physical layer advancements, such as beamforming and massive MIMO (Ghosh et al., 2019).

The propagation characteristics of mmW signals in outdoor environment complicates 5G mmW network design, particularly for broadband application scenarios such as Fixed Wireless Access (FWA). This requires deploying a higher number of cell sites meticulously designed with respect to both terrain and expected user locations data (Medin and Louie, 2019). As in legacy applications of the mmW in backhaul networks, the Line-of-Sight (LoS) signal path between both ends of a wireless link is the key factor in service availability determination. Thus, a practical approach to the complex design problem involves performing LoS assessment between the candidate cell site locations and expected user locations using high-resolution areal survey data.

Light Detection and Ranging (LiDAR) is a remote sensing technology offering very high resolution aerial survey data invaluable in many applications. Becoming popular in recent years, LiDAR has been adopted by operators and software vendors engaged in 5G network design. Basic LoS assessment (aka viewshed or visibility problem) in large terrain environment has been subject of extensive studies in computer science due its relevance to other fields (Floriani and Magillo, 2003).

In this work we present a more comprehensive LoS assessment problem incorporating radio mounting height that is a key practical variable in selecting 5G mmW cell sites. Keeping the required radio-mounting height at minimum leads to significant reduction in the infrastructure cost. Then we propose a new LoS assessment algorithm using LiDAR data that is computationally optimized for the practical aspects of 5G mmW network design. It achieves remarkable

Soosahabi, R. and Bayoumi, M.
Optimized Line-of-Sight Assessment Algorithm for 5G mmW Network Design using LiDAR Information.
DOI: 10.5220/0010548100170024
In *Proceedings of the 18th International Conference on Wireless Networks and Mobile Systems (WINSYS 2021)*, pages 17-24
ISBN: 978-989-758-529-6

computational efficiency compared to the retrofitted LoS assessment algorithms that operate in linear-time complexity at best with respect to the terrain size. Empowered by a novel method to topologically sort terrain data, it takes constant-time, $O(1)$, complexity to execute LoS assessment per user location.

The rest of this article organized as follows: LoS assessment problem investigated in Section 2 followed by Section 3 outlining possible solutions using LiDAR data. Section 4 is designated to mathematical details of proposed algorithm followed by numerical results and conclusion, respectively in Sections 5 and 6.

2 SCOPE OF PROBLEM

This section is dedicated to the practical challenges of designing 5G mmW networks in outdoor environment. Although being used in other wireless applications, the propagation characteristics of mmW signals in outdoor environment poses significant design overhead in terms of infrastructure cost and the computational complexity of coverage prediction models. The problem of LoS assessment using high-resolution terrain data is outlined towards the end of this section. It captures a common design methodology used in current deployments to properly select the radio installation sites.

2.1 Characteristics of mmW Signals

Utilizing mmW frequency bands is a key advancement in 5G new radio (NR) technology. Radios operating in mmW carrier frequency have the luxury of larger transmission bandwidths with smaller antenna elements. Therefore, they can house large antenna arrays in the same form-factor as their sub-6 GHz counterparts. Antenna arrays can be used for creating multiple highly-directional beams for both transmitting and receiving the radio signals. However, mmW radio signals suffer much higher attenuation (path-loss) in the environment compared to their sub-6 GHz counterparts that is attributed to their shorter wavelengths. They cannot penetrate most obstacles nor benefit much from multipath reflections to reach far distances without a LoS signal path. Focusing on the link throughput, some of these propagation losses are compensated for by utilizing higher bandwidth and the beam-forming gains. Presence of LoS signal path coupled with beam-forming can significantly boost per-user throughput and overall cell capacity by enabling SDM (Spatial Diversity Multiplexing) in common point-to-multi-point scenarios. It enables reusing time-frequency resources across multiple beams, given sufficient angular spread among the users. Figure 1 (excerpted from (Medin and Louie, 2019)) depicts the throughput comparison between identical 5G cell deployments in 28 GHz (mmW band) and 3.4 GHz (sub-6 band) in the same serving area, where the red and blue shades respectively denote the maximum achievable throughput in 1.0 Gbps and 100 Mbps ranges. The key observations about 5G cell deployments in mmW band compared to sub-6 band are:

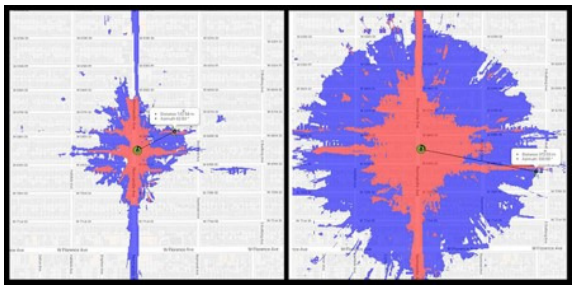

Figure 1: Comparing 5G-NR Coverage: above-6 GHz (left) v.s sub-6 GHz (right) excerpted from (Medin and Louie, 2019). Red and Blue shades indicate high-throughput and low-throughput areas, respectively.

- **Smaller Serving Area Per Cell:** this could be confused as a disadvantage in the first glance, however smaller cells means the achievable cell capacity is divided among fewer users leading to higher average throughput per-user. To cover the same geographical area more cells are deployed with less inter-cell interference, thanks to the fast attenuation of mmW signals. Utility poles and other alternative radio mounting structures are discussed in (Medin and Louie, 2019) as common choices for the operators deploying 5G mmW cells, whereas the technologies in sub-6 bands can still rely on the existing designated telecom towers.
- **Significance of LoS Signal Path:** unlike the sub-6 band, the presence of LoS signal path significantly correlates with service availability. Therefore, the signal quality undergoes drastic variation depending on LoS signal path availability at instantaneous user location, particularly near the cell edge. This phenomenon has already been incorporated in 3GPP standard channel model (3GPP, 2018a) and still subject of study as in (Haneda et al., 2016).

2.2 Design Problem Objectives

Here we consider the problem of designing 5G mmW radio network infrastructure for a given geographic

area without any prior 5G service deployment. There are two typical deployment scenarios: *mobility* and *Fixed-Wireless Access (FWA)*. Mobility services are offered to mobile user devices (UE) while FWA is offering broadband connectivity over mmW links to subscriber devices (CPE) installed on subscribers' properties (typically in sub-urban / rural areas).

The design process in both scenarios starts with collecting: topographical survey information (e.g. terrain, buildings map), property information (e.g. residential, commercial, public venues), and candidate cell deployment sites (e.g. telecom towers, utility poles). Then the desired coverage targets are determined for each scenario considering the following factors:

- **5G Mobility Coverage Targets:** this includes polygons representing the areas with high user density / traffic. Since the users are mobile, there is no need for guaranteed service at any particular location in the polygon. This is a design relief since existing approximate predictions model can still be used to guarantee average service across each polygon.
- **5G FWA Coverage Targets:** Since the wireless link is used to offer broadband services equivalent to wired technologies (e.g. fiber and cable modems), the guarantee of service per user is a more stringent requirement in this scenario. Thus, the service availability for each subscriber property (residential, or commercial) should be individually evaluated in the design phase. there should be at least a CPE installation point on each target property with guaranteed service connectivity.

Although applicable to both scenarios, the proposed solution in this work is optimized more towards the more challenging problem of 5G-FWA design.

Maintaining low *radio mounting height* is another key practical design objective. Depending on CU-DU split scenario (3GPP, 2018b) a combination of directional antennas and other radio hardware components should be mounted on candidate site locations, preferably above the foliage (aka clutter line) to provide connectivity to the surrounding user devices. These hardware components exert structural loads such as wind-loading on their bearing structure (Travanca et al., 2019). The structural load is proportional to the mounting height, so the higher the mounting height, the higher structural reinforcement cost (DeGrasse, 2013). Considering the increased number of cells in 5G mmW and the height and load limitations on the cell candidates (such as utility poles), the structural cost can become prohibitive without controlling the mounting height in the design phase.

The 5G mmW design problem is a complex integer programming task whose output includes a set of cell site coordinates, mounting height and the angular orientation of antennas.

2.3 LoS Assessment Problem

As stated in Section 2.1, Existence of LoS signal path between the user devices and the serving radio can be accounted as a reliable service availability metric. This evidently becomes a trade-off based on the fact that the higher the mounting height, the more user locations with LoS signal path (Haneda et al., 2016). Hence, a solution to the sophisticated cellular design problem will depend on solving the following problem for each cell site candidate:

Problem 1. ***(LoS Query):*** *For a given cell deployment coordinate (on XY-plane) and any user location point (in XYZ-space), compute the minimum radio mounting height at the cell site (minRMH) to achieve LoS between the user and the cell radio.*

Computing *minRMH* for every combination of candidate site location and user point is a prerequisite to any design decision. Solving Problem 1 requires very high-resolution *Digital Elevation Model* (DEM) of the serving area that come in considerable data volumes. Hence, any solution algorithm should be efficient in terms of computation complexity per query since this computation can be repeated in several iterations per each cell site candidate through the design process.

3 SCOPE OF SOLUTION

This section details the required data source and the process to solve Problem 1, including: geometric formulation of LoS problem in terms of *minRMH* and they elements of the existing and proposed algorithms.

3.1 Creating DEM from LiDAR Data

Light Detection and Ranging (LiDAR) offers comprehensive areal survey data with very high resolution suited for accurate LoS assessment. It is a high-resolution remote sensing technology using the pulsed laser transceiver typically mounted under an aircraft to scan the surface below a raster flight path. Similar in concept to radar technology, the characteristics of the returned pulses are used to estimate the coordinates of the reflection points. The output of raw LiDAR scan is commonly called a *point-cloud*

which is a scattered set of 3D points (in UTM coordinate system) (Wandinger, 2005). Projected in 3D XYZ-space, the points are distributed almost uniformly on XY-plane (base-plane) with a fixed step size. Due to its high demand in various survey applications in some countries, the government agencies (e.g. (USGS, 2018)) collect and publicly distribute LiDAR data on periodic basis for most of the areas.

The raw LiDAR data are normalized and presented in the form of a Cartesian DEM to study the elevation information, where Z-axis values show the elevation across the base plane. An example of outdoor DEM displayed in Fig. 2. In each iteration of LoS assessment, the candidate cell site is usually mapped to the origin of XY-plane with possible radio mounting points along the Z-axis.

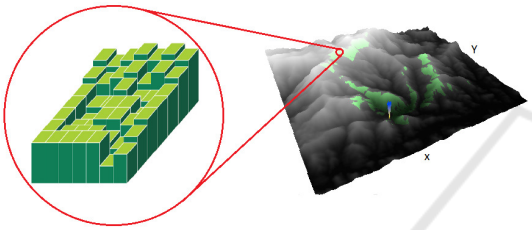

Figure 2: Example of outdoor DEM.

LiDAR provides ample resolution compared to common clutter models using terrain approximation. For example, the public data provided by USGS offers $70cm$ leading to a DEM with an enormous data set in most survey projects. Therefore, efficient algorithms are required to perform LoS assessment task. DEMs representing LiDAR data have disproportionate value range across their dimensions. In a Cartesian system, expanding the area under study pushes the limit along X-axis and Y-axis in the scales of kilometers, while the elevations along Z-axis remain within the range of hundreds of meters in most topographies.

Remark. *To incorporate the scale of DEM size in algorithm complexity notation, it is modeled as an $N \times N$ grid of elevation values quantized into K digital levels. In the subsequent analysis, the algorithmic complexities are expressed in orders of N while K is considered an $O(1)$ constant.*

3.2 LoS Assessment Geometry

Problem 1 is a classic 3D visibility problem that can be reduced to a 2D sub-problem in the following section.

3.2.1 Creating 2D Sub-problem

Considering a DEM in Cartesian space where the radio mounted along "Z-axis, a *ray* is a line connecting a point on the Z-axis to a user location under study. This ray together with the Z-axis will form a half-plane that we refer to as a *ray-plane*. A ray indicates a LoS (visibility) condition, if it is not obstructed with any other DEM object in between its two end-points. Hence, examining the DEM points residing on the ray-plane should be sufficient to determine LoS condition. More sophisticated propagation models evaluate LoS conditions for a cluster of rays to predict signal levels which is outside the scope of this work. Since the ray-plane will always be perpendicular to the XY-plane (base-plane), it is simple to identify the DEM points intersecting with the ray-plane by projecting the ray onto XY-plane and selecting the DEM grid points it crosses. Once selected through this process, the DEM points on the ray-plane can be represented in a new 2D Cartesian coordinate system $X'Z$, where a values on X'-axis shows the distance of the point from the Z-axis, and the Z values are preserved as the radio mounting height. An example of ray-plane has been illustrated in Fig. 3 constructed with Z-axis and a DEM point P_m.

Henceforth, $\mathcal{P} = \{P_0, P_1, P_2, \cdots, P_N\}$ denotes an enumerated set of N DEM points $P_j = (x'_j, z_j)$ in a ray-plane indexed in asceding order according to their x'_j values for $0 \leq j \leq N$. The origin is fixed at P_0 and P_N denotes farthest point along the X' axis, i.e. the horizon. Here we assume that all elevation values are normalized by the lowest possible value. The base ground elevation is assumed to be 0.

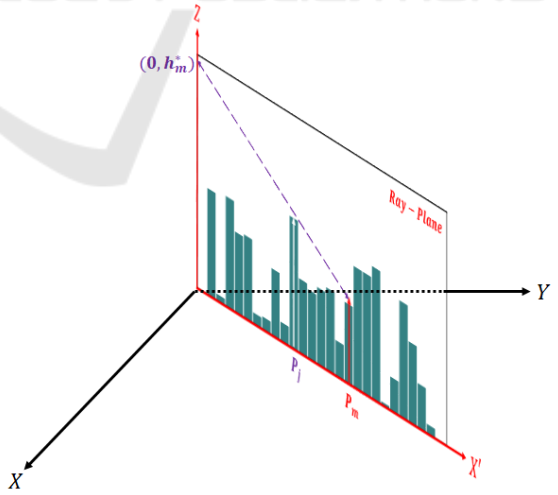

Figure 3: Visualizing the ray-plane and a solution for Problem 2.

Now the LoS query problem for each point in the ray-plane can be formulated as:

Problem 2. ***(2D LoS Query):*** *Given the set of ray-plane points $\mathcal{P}$, and a point $P_m \in \mathcal{P}$, compute the*

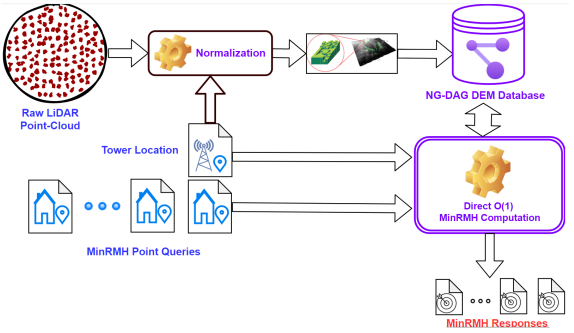

Figure 4: Proposed LoS assessment algorithm.

minRMH value h^*_m to reach LoS between the pair of points: P_m and $(0,h^*_m)$ on $X'Z$-plane.

The value h^*_m should be computed such that none of the intermediate DEM points appear above the line connecting $(0,h^*_m)$ to P_m. The minimality condition implies that there would be at least a DEM point P_j with $0 < j < m$ barely residing on this line. The dashed purple line in Fig. 3 demonstrates an example solution to Problem 2.

3.2.2 Solving 2D Sub-problem

One can show that each point independently contributes in the value of h^*_m. Let $h^*(m,j)$ denote the *minRMH* for P_m given the condition that all the intermediate points are eliminated except P_j, $0 < j < m$. One can draw a line connecting P_m and P_j representing the ray which barely meets LoS. Extending this line towards Z axis lands at $(0,h^*(m,j))$, where

$$h^*(m,j) = \frac{z_j x'_m - z_m x'_j}{x'_m - x'_j} \quad (1)$$

. Applying the max-min technique, it can be shown that

$$h^*_m = max\{h^*(m,i)\}_{i=1}^{m-1} \quad (2)$$

3.3 Using Existing Visibility Algorithms

Discovering LoS for pairs of points in a 3D space is a classic computational geometry problem with wide-ranging applications (Floriani and Magillo, 2003). The most common algorithms are optimized to compute what known as *viewshed*, where all the points in a DEM with LoS path to a single point are discovered. They are not optimized to accurately compute *minRMH* queries as articulated in Problem 1. Repurposing viewshed algorithms for this problem may require iteratively computing viewshed for all possible radio-mounting values, in $O(K)$, and extracting *minRMH* for user locations. In doing so, one of the best known algorithm developed by Van Kreveld in (Van Kreveld, 1996) that results in a solution complexity in order of $O(KN^2logN)$.

R3 algorithm proposed in (Sorensen and Lanter, 1993) is one of the early algorithms that operates in query fashion and can be modified to solve Problem 2. The computational complexity of (2) is $O(N)$ per query since (1) should be computed for all the preceding points to P_m. Put in perceptive to (Van Kreveld, 1996), computing *minRMH* for the entire DEM using R3 will result in $O(N^3)$ complexity.

3.4 Elements of Proposed Algorithm

The proposed algorithm is optimized to process the Problem 2 queries in constant time, $O(1)$, independent to the distance of the query point from the tower location, proportional to N. Exhaustively solving (2) for all the DEM points in a ray-plane leads to a $O(N^2)$ complexity. The key distinction of the proposed algorithm is using a fast-constructable data structure in form of a *Directed Acyclic Graph (DAG)* to reduce computation complexity of (2). As illustrated in Figure 4, the proposed algorithm comprised of and extra offline processing step to construct the DAG and an online query-handling process.

The reprocessing steps starts with common data normalization and DEM creation. Then given the candidate cell site location, the DEM points are grouped into a set of possible ray-planes. The set of all possible ray-planes can be created by considering each point at the fringe of the DEM and the cell site at the origin. Then each ray-plane independently undergoes DAG construction process.

The query handling consists of two steps: ray-plane determination and *minRMH* computation. The first step requires a simple ray-plane look-up based on the angular orientation of the query point on the base plane. The second step involves computing (1) for a collection of points while traversing the pre-constructed ray-plane DAG.

4 Proposed Algorithm

The key elements of proposed LoS assessment algorithm are detailed in this section by focusing on the components of an optimal solution to Problem 2 within a given ray-plane.

4.1 DAG Construction

The following proposition provides the key insight to skip the redundant iteration in (2).

Proposition 1. *Given a point Pm* $\in \mathcal{P}$ *and a pair of its preceding points* P_i *and* P_j *such that* $0 < x'_i < x'_j < x'_m$, *satisfying* $h^*(m,i) > h^*(m,j)$ *requires* $z_i > z_j$.

It is straightforward to prove Proposition 1 using the formula in (1). Since the max operation is used across $h^*(m,i)$ values to compute h^*_m, this can be used in its negative form to ignore points that produce insignificant $h^*(m,i)$ values. Starting from P_m and iterating backwards to P_0, after computing $h^*(m,j)$ for a point P_j, we shall jump to computing $h^*(m,i)$ for the next preceding point P_i with greater elevation $z_i > z_j$. We need to continue these jumps until there is no preceding point with higher elevation. This can save lots of computation cycles by skipping low intermediate points in between the jumps. Since this operation may be repeated to compute *minRMH* for any points in a ray-plane, it would be beneficial to determine the preceding higher point to each point in a single preprocessing step. This will be a simple variation of the classic nearest smallest point problem in computer science, where extremely efficient solution algorithms are available in (Berkman et al., 1993) and (Berkman et al., 1998).

In the context of a ray-plane, the enumerated set of points in $\mathcal{P}$ are augmented in the format of $P_i = (x'_i, z_i, p_i)$ for $0 < i \leq N$, where p_i stands for a pointer (index) the next-greater-elevation-point (NGP) preceding P_i. In each ray-plane there could be some peak points where $p_i = Null$, implying the minimum radiation center be zero. The augmented $\mathcal{P}$ can be graphically represented as a DAG demonstrated in Fig. 5, where the blue arrows show the added pointers, i.e. DAG edges.

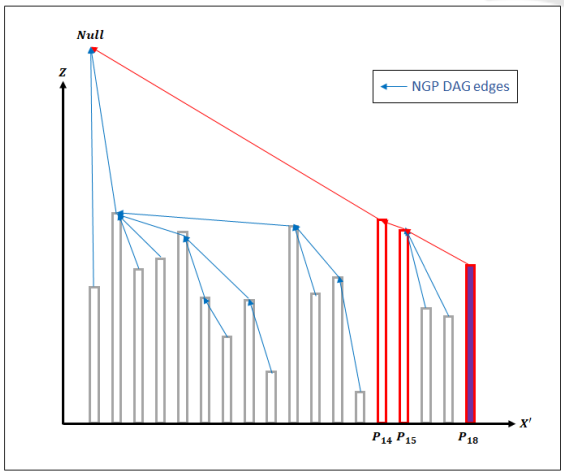

Figure 5: NGP-DAG visualization in a ray-plane.

4.2 DAG Traversal

After constructing the DAG for a given ray-plane with augmented point set $\mathcal{P}$, the minimum radiation center h^*_m is computed for each $P_i \in \mathcal{P}$ by only traversing DAG predecessors of P_i and computing (1) whose maximum value reported as *minRMH*. This procedure is outlined in Algorithm 1.

The red arrows in Fig. 5 depict the DAG traversal path to compute *minRMH* for a sample point P_{18}. It shows that Problem 2 can be efficiently solved in 2 iterations (evaluating (1) for P_{15} and P_{14}) using the proposed algorithm, whereas an exhaustive algorithms requires 17 iterations to evaluate (1) for all the points P_1 to P_{17}.

Algorithm 1: Proposed DAG-traversal Algorithm.

```
1: procedure (2D LoS Query): P_m, P
2:     h*_m ← 0
3:     i ← m
4:     while p_i ≠ Null do
5:         h*_m ← max(h*(m,i), h*_m)
6:         i ← p_i
7:     end while
8:     return h*_m
9: end procedure
```

4.3 Complexity Analysis

Using the algorithm outlined in (Berkman et al., 1993) the DAG can be constructed in a near-constant time $O(loglogN)$ one-shot operation that can be further improved to an absolute constant order $O(logloglogK)$ utilizing a hyper-threaded computing environment (Berkman et al., 1998).

The complexity of the Algorithm 1 determined by the expected number of the while-loop iterations. The loop continues as long as there is an NGP with higher elevation. Therefore, the total number of loop iterations is bounded by the constant K, the number of possible elevation levels in the DEM. It can be shown that the expected number of loop iterations is relative to the expected length of the underlying longest-increasing-sequence of elevations in each ray-plane, proved to be $O(\sqrt{K})$ in (Odlyzko and Rains, 2000).

Remark. *Combining the two steps, the proposed algorithm achieves a constant-time* $O(\sqrt{K})$ *solution to compute minRMH queries in Problem 1.*

This algorithm can also be used to compute *minRMH* for the entire DEM points (*viewshed mode*) in some scenarios such as mobility applications in municipal areas. The table in Figure 6 summarizes the performance of the proposed algorithm compared to the existing algorithms discussed in Section 3.3 for both scenarios.

Algorithm	Query Complexity	Viewshed Complexity
R3	$O(N)$	$O(N^3)$
Van Kreveld's	N/A	$O(KN^2logN)$
Proposed	$O(\sqrt{K})$	$O(\sqrt{K}N^2)$

Figure 6: Algorithms' computational complexities.

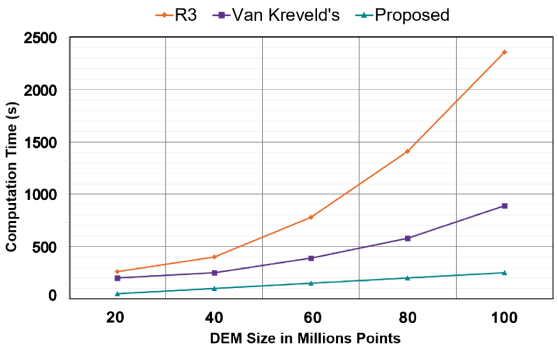

Figure 7: Comparing execution time of the algorithms.

5 NUMERICAL RESULTS

In this section, we present the implementation details for the proposed LoS Assessment algorithm for a commercial 5G-FWA deployment scenario. Then compare the computation time with the existing algorithms described in Section 3.3 in the same settings to demonstrate the predicted efficiency gains.

5.1 Test Environment

The public LiDAR data set for a suburban residential neighborhood in the central area of the State of Mississippi are obtained from Mississippi Automated Resource Information System (MARIS) at (Woolpert, 2014). All algorithms are implemented in C++14 using PDAL (`https://pdal.io`) utility API to preprocess the LiDAR data set and create a basic DEM. The subsequent codes are compiled with `gcc -Ofast` utility into executable libraries. The run-time environment hosted on a RHEL® Linux virtual machine with access to 16 GB of RAM and 2 Intel XEON® processors.

5.2 Test Scenario

The DEM has been created for a maximum of 8 km radius area around a cell tower of maximum height 60 m as a potential deployment site for 5G FWA in *n*257 band (28 GHz). To achieve a fair comparison with (Van Kreveld, 1996), the analysis is performed in viewshed mode for the proposed algorithm and R3 in (Sorensen and Lanter, 1993). We have computed *minRMH* for all the DEM points within a circle centered at the origin with different radii to achieve different number of point queries shown Figure 7. The execution time in seconds has been plotted in Figure 7 for all 3 algorithms for different number of DEM points. Considering the values in horizontal axis is proportional to N^2, the execution times follow the expected complexity trends indicated in Figure 6 table for the viewshed scenario.

6 CONCLUSION

Considering the practical challenges of 5G mmW network design, we present a comprehensive LoS assessment problem incorporating radio mounting height. Then we propose a new LoS assessment algorithm using LiDAR data that is computationally optimized for the practical aspects of 5G mmW network design. Empowered by a novel method to topologically sort terrain data, it achieves constant-time, $O(1)$, complexity to execute LoS assessment per user location, whereas the complexity of retrofitted LoS algorithms for the same task grows linearly, $O(1)$ with respect to the data dimensions. The improvements in the run-time efficiency are verified in numerical results for a real deployment scenario. It is worth investigating means of leveraging this algorithm to reduce the computational complexity of coverage prediction algorithms based on ray-tracing.

ACKNOWLEDGMENTS

We would like to express our appreciation to Infolink-USA Inc. staff for providing the opportunity to study the practical challenges in deploying 5G-FWA networks and motivating us to deploy our solution as a joint venture with their clients.

REFERENCES

3GPP (2018a). LTE; 5G; Study on channel model for frequency spectrum above 6 GHz. Technical Specification (TS) 38.900, 3rd Generation Partnership Project (3GPP). Version 15.0.0.

3GPP (2018b). Study on Central Unit (CU) - Distributed Unit (DU) lower layer split for NR. Technical Specification (TS) 38.816, 3rd Generation Partnership Project (3GPP). Version 15.0.0.

Berkman, O., Matias, Y., and Ragde, P. (1998). Triply-logarithmic parallel upper and lower bounds for minimum and range minima over small domains. *Journal of Algorithms*, 28(2):197–215.

Berkman, O., Schieber, B., and Vishkin, U. (1993). Optimal doubly logarithmic parallel algorithms based on finding all nearest smaller values. *Journal of Algorithms*, 14(3):344–370.

DeGrasse, M. (2013). Tower loading challenges wireless infrastrucure providers. https://www.rcrwireless.com/20131002/network-infrastructure/tower-loading-challenges-wireless-infrastrucure-providers. Accessed: 2017-09-30.

Floriani, L. and Magillo, P. (2003). Algorithms for visibility computation on terrains: a survey. *Environment and planning B: Planning and design*, 30(5):709–728.

Ghosh, A., Maeder, A., Baker, M., and Chandramouli, D. (2019). 5g evolution: A view on 5g cellular technology beyond 3gpp release 15. *IEEE Access*, 7:127639–127651.

Haneda, K., Zhang, J., Tan, L., Liu, G., Zheng, Y., Asplund, H., Li, J., Wang, Y., Steer, D., Li, C., et al. (2016). 5g 3gpp-like channel models for outdoor urban microcellular and macrocellular environments. In *2016 IEEE 83rd vehicular technology conference (VTC spring)*, pages 1–7. IEEE.

Medin, M. and Louie, G. (2019). The 5g ecosystem: Risks and opportunities for dod. Technical report, Defense Innovation Board Washington DC United States.

Odlyzko, A. and Rains, E. (2000). On longest increasing subsequences in random permutations. *Contemporary Mathematics*, 251:439–452.

Sorensen, P. A. and Lanter, D. (1993). Two algorithms for determining partial visibility and reducing data structure induced error in viewshed analysis. *Photogrammetric Engineering and Remote Sensing*, 59:1149–1160.

Travanca, R., de J. Souza, T., and André, J. (2019). Structural safety assessment of 5g network infrastructures. *Wiley 5G Ref: The Essential 5G Reference Online*, pages 1–21.

USGS (2018). Lidar Base Specification. Standard 11-B4, U.S. Geological Survey Standards. Version 1.3.

Van Kreveld, M. (1996). *Variations on sweep algorithms: efficient computation of extended viewsheds and class intervals*, volume 1996. Utrecht University: Information and Computing Sciences.

Wandinger, U. (2005). Introduction to lidar. In *Lidar*, pages 1–18. Springer.

Woolpert (2014). United States Geological Survey NRCS Laurel MS 0.7 NPS LIDAR. https://www.maris.state.ms.us/HTML/DATA/data_Elevation/REPORTS/Lidar%20Rpt_USGS%20LaurelMS%20Lidar_Dec2014.pdf.